A Second Magnesium Ion Is Critical for ATP Binding in the Kinase Domain of the Oncoprotein v-Fps†

Phillip Saylor, Chengqian Wang, T. John Hirai, and Joseph A. Adams*

Department of Chemistry, San Diego State University, San Diego, California 92182-1030

Received May 28, 1998; Revised Manuscript Received July 10, 1998

ABSTRACT: The activity of the kinase domain of the oncoprotein v-Fps was found to be sensitive to the concentration of magnesium ions. Plots of initial velocity versus free magnesium concentration are hyperbolic and do not extrapolate to the origin at stoichiometric ATP-Mg, indicating that there are two sites for metal chelation on the enzyme and the second is nonessential for catalysis. The second metal is strongly activating and increases the reaction rate constant almost 20-fold from 0.5 to 8.3 s^{-1} using 0.2 mM ATP-Mg and 1 mM peptide, EAEIYEAIE. This increase in rate is due to a large increase in the apparent affinity of ATP-Mg at high magnesium concentrations. At 0.5 and 10 mM free Mg^{2+}, K_{ATP-Mg} is 3.6 and 0.22 mM, respectively. Extrapolation of the observed affinity of ATP-Mg to zero and infinite free metal indicates that K_{ATP-Mg} is greater than 8 mM in the absence of the second metal and 0.1 mM in the presence of the second metal, a minimum 80-fold enhancement. By comparison, free levels of the divalent ion do not influence maximum turnover (k_{cat}) and have only a 2-fold effect on the K_m for the peptide substrate between 0.5 and 20 mM free Mg^{2+}. Viscosometric studies indicate that free Mg^{2+} does not influence the rates of phosphoryl transfer or net product release above 0.5 mM but does affect directly the dissociation constant for ATP-Mg. The K_d for ATP-Mg in the absence and presence of the second metal ion is >32 and 0.4 mM, respectively. At high magnesium concentrations, ATP-Mg and the peptide substrate bind independently, while at lower concentrations (0.5 mM), there is significant negative binding synergism suggesting that the second metal may help to reduce charge repulsion between ATP-Mg and the peptide. The data indicate that the first metal is sufficient for phosphoryl transfer. While the second metal could have some influence on phosphoryl transfer or product binding, it is a potent activator that functions minimally by controlling ATP-Mg binding.

Protein phosphorylation is catalyzed by a large class of enzymes known as protein kinases. They are characterized by a number of features including their substrate specificity. Protein kinases that phosphorylate serine and threonine residues are called protein serine kinases (PSKs),[1] and those that phosphorylate tyrosine are known as protein tyrosine kinases (PTKs). The former class is mostly cytoplasmic in localization, while the latter class is either integral membrane or cytoplasmic proteins. All protein kinases utilize a nucleoside triphosphate, normally ATP, to deliver a phosphoryl group to the hydroxyl acceptor. The activity of these enzymes is greatly affected by the nature and concentration of an essential divalent metal ion (*1*−*6*). While many protein kinases are active in the presence of several divalent metals, they are usually most active in the presence of Mg^{2+}, and since the concentration of this ion exceeds those of others in the cell, Mg^{2+} is considered the true physiological metal for the protein kinases. It has been shown for cAMP-dependent protein kinase (PKA), a PSK, that two metal ions modulate enzymatic activity. The first metal chelates the $\beta\gamma$ phosphates of ATP and is essential for activity, while the second metal chelates the $\alpha\gamma$ phosphates and represses turnover by 4-fold (*1*, *3*, *7*). The latter effect may be due to changes in the release rate of ADP, the rate-determining step in turnover at high magnesium concentrations (*8*). In support of these findings, the affinity of both ATP and ADP increase at high concentrations of free Mg^{2+} (*3*, *4*, *9*).

While it is clear that other protein kinases are influenced by the concentration of metal ions, it is not clear whether there is a general trend shared by all enzymes within the family. Also, it is not clear which step or steps in the kinetic mechanism are affected. For example, it was recently demonstrated that the steady-state kinetic parameters of the nonreceptor PTKs, Csk and Src, are affected differently than those for PKA. K_{ATP-Mg} is not altered by the amount of free Mg^{2+} for either of these PTKs, although V_{max} increases substantially as the second metal binds (*10*). It has been suggested that PTKs may respond differently to metal ion concentration depending on whether these enzymes are receptor or nonreceptor PTKs. In support of this conclusion, K_{ATP-Mg} decreases with increasing Mg^{2+} for both receptor PTKs, IRK and FGFR (*10*, *11*).

The response of catalytic activity to metal ion concentration in the nonreceptor PTKs may be further influenced by

† This work was supported by NIH Grant CA 75112 and by the California Metabolic Research Foundation.

* To whom correspondence should be addressed. Tel: (619) 594-6196. Fax: (619) 594-1879. E-mail: jadams@sundown.sdsu.edu.

[1] Abbreviations: Csk, C-terminal Src kinase; FGFR, fibroblast growth factor receptor PTK; GST, glutathione-*S*-transferase; Mops, 3-(*N*-morpholino)propanesulfonic acid; PKA, cAMP-dependent protein kinase; PSK, serine-specific protein kinase; PTK, tyrosine-specific protein kinase; v-Fps, nonreceptor PTK of the Fujinami sarcoma virus.

S0006-2960(98)01267-7 CCC: $15.00
Published on Web 08/19/1998

neighboring subdomains such as SH2 and SH3 domains or by regulatory phosphorylation events outside the kinase domain. To demonstrate whether there are inherent differences in the metal ion response for receptor and nonreceptor PTKs, it is essential to study the kinase domain of a nonreceptor PTK free of its regulatory components and to assess the effects of metal ions with respect to the individual steps in the phosphoryl transfer mechanism. We have previously expressed and purified a highly active form of the kinase domain of the oncoprotein v-Fps, a member of the Fps/Fes family of nonreceptor PTKs (*12*). This isolated kinase domain, which was purified as a GST fusion protein, is autophosphorylated in bacteria (*12*) and has a turnover number that is close in value to that for the highly active catalytic subunit of PKA (*13*, *14*). We demonstrated that this kinase domain is strongly activated by free $Mg^{2+}$and this activation is due to large decreases in K_{ATP-Mg} at higher metal concentrations with no changes in turnover number between 0.5 and 20 mM free magnesium. We identified the individual steps affected by this second metal using viscosometric techniques.

MATERIALS AND METHODS

Materials. Adenosine 5′-triphosphate (ATP), phosphoenolpyruvate, magnesium chloride, nicotinamide adenine dinucleotide, reduced (NADH), tris(hydroxymethyl)aminomethane (Tris), 3-(*N*-morpholino)propanesulfonic acid (Mops), pyruvate kinase, type II, from rabbit muscle, and lactate dehydrogenase, type II, from bovine heart, were purchased from Sigma. Ethylenediaminetetraacetic acid (EDTA) and dithiothreitol (DTT) were purchased from Fisher.

Peptides and Protein. The peptide substrate EAEIYEAIE was synthesized by the USC Microchemical Core Facility using Fmoc chemistry and purified by C-18 reverse-phase HPLC. The concentration of the peptide was determined by weight. The fusion protein GST-kin was purified from *Escherichia coli* according to previously published procedures (*12*, *13*). The total concentration of the protein eluted from the glutathione agarose affinity resin was determined by a Bradford assay. While the protein preparation contains no free kinase domain, some cleaved GST is present. The concentration of fusion protein (usually 20−30%) was determined by gel densitometry. The enzyme was stored at −70 °C in a buffer containing 50 mM Tris (pH 7.5), 1 mM EDTA, 150 mM NaCl, 1 mM DTT, and 10% glycerol. The enzyme was thawed on ice (4 °C) and used immediately for each kinetic study.

Kinetic Assay. The enzymatic activity of GST-kin was measured spectrophotometrically using a coupled enzyme assay. This assay couples the production of ADP with the oxidation of NADH using pyruvate kinase and lactate dehydrogenase. In general, varying amounts of peptide were mixed manually with varying ATP (0.1−10 mM), varying $MgCl_2$, and 0.06−0.42 μM GST-kin in a 50-μL (minimum volume) quartz cuvette containing 0.40 mM phosphoenolpyruvate, 0.20 mM NADH, 2 units of lactate dehydrogenase, and 0.5 unit of pyruvate kinase. The total concentration of $MgCl_2$ needed to obtain a desired free concentration of Mg^{2+} was calculated based on the dissociation constants of 0.0143 mM for ATP-Mg, 5 mM for Mg-PEP, and 19.5 mM for Mg-NADH (*15*). All reactions were measured in a Beckman DU640 spectrophotometer equipped with a microcuvette holder in a buffer containing 50 mM Mops at pH 7.0, in a final volume of 60 μL at 23 °C. Absorbance changes at 340 nm were collected over a time range of 100−200 s. Less than 10% of the substrate peptide was consumed in each initial velocity measurement. All initial velocities varied linearly with the concentration of the fusion protein.

Viscosometric Measurements. The relative solution viscosities (η^{rel}) of buffers containing glycerol were measured relative to a standard buffer of 100 mM Mops, pH 7.0, at 23 °C, using an Ostwald viscometer (*16*). Each viscosity measurement was carried out using 5.0 mL of buffer containing varying amounts of viscosogen. The amount of time required for each buffer to move through the markings on the viscometer was recorded. The relative viscosity of each buffer was calculated using eq 1:

$$\eta^{rel} = \frac{t\,(\%)}{t} \times \frac{\rho\,(\%)}{\rho} \tag{1}$$

where η^{rel} is the relative solvent viscosity, t (%) and t are the transit times for a given viscous buffer and the standard buffer, respectively, and ρ (%) and ρ are the densities of the viscous and standard buffers, respectively. The following relative solvent viscosities were obtained for the buffers (% viscosogen, η^{rel}): 35% glycerol, 3.7; 27% glycerol, 2.8; 20% glycerol, 2.1. All solvent viscosity measurements were performed in triplicate and did not deviate by more than 4% in value.

Data Analysis. The initial velocity data were measured as a function of either free Mg^{2+} at fixed ATP-Mg and peptide substrate or variable peptide substrate at fixed, varied ATP-Mg and fixed free Mg^{2+}. The steady-state kinetic parameters at each concentration of free Mg^{2+} were measured at varying peptide and varied, fixed ATP-Mg using eq 2:

$$v = \frac{V_{max}[S]}{K_{peptide}\left(1 + \frac{K_{iATP-Mg}}{[A]}\right) + [S]\left(1 + \frac{K_{ATP-Mg}}{[A]}\right)} \tag{2}$$

where v and V_{max} are the initial and maximum velocities, $K_{peptide}$ and K_{ATP-Mg} are the observed Michaelis constants for peptide substrate and ATP-Mg, and $K_{iATP-Mg}$ is the dissociation constant for ATP-Mg. The maximum rate constant, k_{cat}, was determined from V_{max} and the enzyme concentration. The observed values of K_{ATP-Mg} determined from eq 2 were plotted as a function of free Mg^{2+}, and the data were fit to eq 3:

$$K_{ATP-Mg} = \frac{{}^{*}K_{ATP-Mg}[Mg^{2+}] + {}^{\circ}K_{ATP-Mg}K_{Mg}}{[Mg^{2+}] + K_{Mg}} \tag{3}$$

where ${}^{*}K_{ATP-Mg}$ is K_{ATP-Mg} when the second metal is bound, K_{Mg} is the observed affinity of the second metal, and ${}^{\circ}K_{ATP-Mg}$ is K_{ATP-Mg} with only one metal bound.

RESULTS

Effects of Free Magnesium on Initial Velocity. The initial velocity of the enzyme reaction was monitored as a function of free Mg^{2+} at fixed concentrations of ATP-Mg and peptide

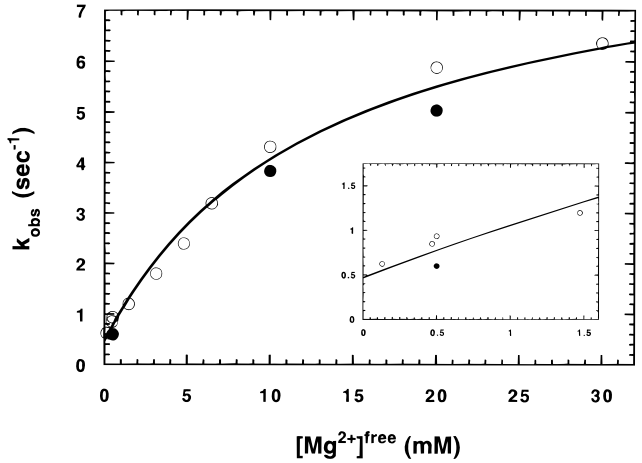

FIGURE 1: Initial reaction rate constants (k_{obs}) for the phosphorylation of EAEIYEAIE (1 mM) as a function of free Mg^{2+} using 0.2 mM ATP and 0.14−0.42 μM GST-kin (○). The total concentration of $MgCl_2$ ranged from 0.35 to 30.5 mM. The data were fit to a hyperbolic function where the reaction rate constants ($k_{obs} = v/[E]$) at zero and infinite free Mg^{2+} are 0.47 ± 0.12 and 8.3 ± 0.50 s^{-1}, respectively, and the concentration for half-maximal velocity is 13 ± 2.5 mM. The predicted values of the initial reaction rate constants (●) at 0.5, 10, and 20 mM free Mg^{2+} based on the steady-state kinetic parameters are also shown. The inset shows the rate constant data and fit at low free Mg^{2+} concentrations (<1.5 mM).

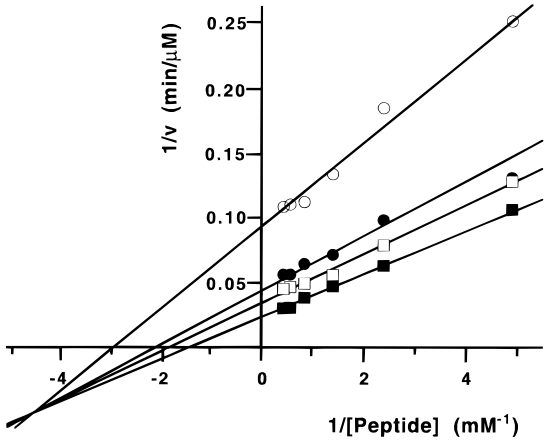

FIGURE 2: Double-reciprocal plot of initial velocity versus peptide concentration at varied, fixed ATP-Mg concentrations using 0.5 mM free Mg^{2+}. Initial velocities were measured using 0.1−3 mM EAEIYEAIE, 0.060 μM GST-kin, and 1 (○), 2 (●), 5 (□), and 10 (■) mM ATP. The total concentration of $MgCl_2$ ranged from 1.5 to 10.3 mM.

substrate. A plot of initial velocity versus free Mg^{2+} is shown in Figure 1 using 0.2 mM ATP, 1 mM peptide substrate, and 0.14−0.42 μM GST-kin. The reaction rate constant ($v/[E]$) increases hyperbolically with increasing free metal. The data were fit to a hyperbolic function with a non-zero intercept. The fitting of these data provides initial rate constants of 0.47 ± 0.12 and 8.3 ± 0.50 s^{-1} at zero and infinite concentrations of free Mg^{2+}, respectively. The half-maximal rate constant corresponds to a free metal concentration of 13 ± 2.5 mM. The inset to Figure 1 shows the low metal concentration data. On the basis of the stability constant of Mg-ATP (0.0143 mM), the total concentration of ATP closely approximates the concentration of Mg-ATP at and above 0.5 mM free Mg^{2+} but the concentration of free ATP increases below this limit. For example, at 0.1 and 0.5 mM free Mg^{2+} approximately 88% and 95% of the total ATP (0.2 mM) is bound with magnesium. Background reactions were measured at each concentration of free Mg^{2+} by measuring the initial reaction velocity in the absence of peptide substrate. These background rates at the lowest metal concentrations (≤1 mM) were less than 20% of the reaction velocity in the presence of the peptide substrate and were subtracted from the observed rates. The background rates above 3 mM free Mg^{2+} were less than 5% of the observed reaction rates.

Steady-State Kinetic Parameters as a Function of Free Magnesium. The steady-state kinetic parameters for the phosphorylation of the peptide were monitored at a series of fixed, free Mg^{2+} concentrations. The parameters were determined by measuring the initial velocities of the reaction as a function of varying peptide concentration (0.1−3.5 mM) at varied, fixed concentrations of ATP-Mg (0.1−10 mM). A typical double-reciprocal plot at 0.5 mM free Mg^{2+} is shown in Figure 2. The lines intersect below the 1/[S] axis indicating that the binding of one ligand impedes the binding of the second. At higher concentrations of free Mg^{2+}, this effect becomes less pronounced and the lines intersect closer to the 1/[S] axis (data not shown). The data were analyzed using eq 2, and the parameter fits are shown in Table 1 at 0.5 and 10 mM free Mg^{2+}. The steady-state kinetic parameters were also measured at other concentrations of free Mg^{2+}, and the results of these fits are plotted in Figure 3. Free metal did not influence the turnover number for the enzyme (not shown in plot) and had only a small effect on the observed K_m for peptide (2-fold). In contrast, the observed K_{ATP-Mg} decreased significantly with increasing free metal. These data were fit to eq 3 to obtain the following fits: $*K_{ATP-Mg} = 0.10 \pm 0.07$ mM, $°K_{ATP-Mg} > 8$ mM, $K_{Mg} < 0.3$ mM. Only lower and upper limits could be placed on K_{ATP-Mg} and K_{Mg}, respectively, since it is not possible to go lower than 0.5 mM free Mg^{2+} without generating large amounts of free ATP (see previous section). Finally, it was shown previously that the kinetic parameters for GST-kin are identical in the presence and absence of 50 mM NaCl indicating that changes in ionic strength at high ATP levels are not the source of any rate effects (*13*, *17*).

Table 1: Steady-State Kinetic Parameters for the Kinase Domain of v-Fps at 0.5 and 10 MM Free Magnesium[a]

parameters	[Mg^{2+}]^{free} (mM) 0.5[b]	10[c]
k_{cat} (s^{-1})	16 ± 2	14 ± 1.7
$K_{iATP-Mg}$ (mM)	0.90 ± 0.20	0.17 ± 0.04
K_{ATP-Mg} (mM)	3.6 ± 0.10	0.22 ± 0.02
$K_{peptide}$ (mM)	0.90 ± 0.10	0.54 ± 0.07

[a] The steady-state kinetic parameters were measured in 100 mM Mops, pH 7, at 23 °C. [b] These kinetic parameters were measured from plots of initial velocity versus varying peptide substrate concentrations (0.1−3.5 mM) at varied, fixed levels of ATP (1−10 mM). The total concentration of GST-kin was 0.06 μM, and $MgCl_2$ ranged from 1.5 to 10.3 mM. [c] These kinetic parameters were measured from plots of initial velocity versus varying peptide substrate concentrations (0.1−3.5 mM) at varied, fixed levels of ATP (0.1−2 mM). The total concentration of GST-kin was 0.06 μM ,and $MgCl_2$ ranged from 10.4 to 12.3 mM.

Viscosity Effects on the Kinetic Parameters at 0.5 and 10 mM free Magnesium. The steady-state kinetic parameters were measured as a function of solvent viscosity at 0.5 and 10 mM free Mg^{2+}. The initial velocity of the reaction was

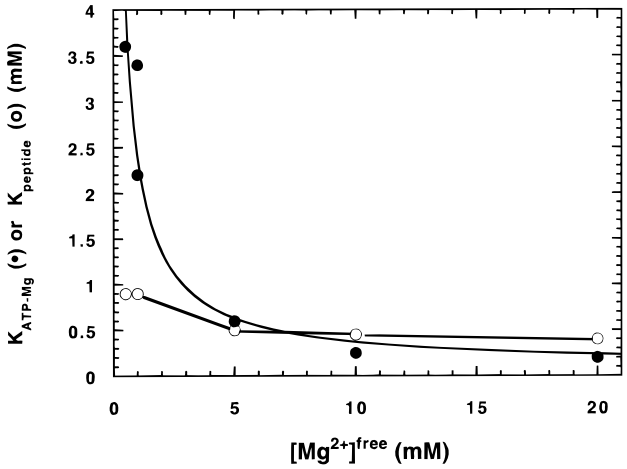

FIGURE 3: Apparent K_m values for ATP-Mg, K_{ATP-Mg} (●), and EAEIYEAIE, $K_{peptide}$ (○), as a function of free Mg^{2+}. The apparent K_m values were measured using eq 2, and the metal dependence on K_{ATP-Mg} was fit to eq 3 to obtain $°K_{ATP-Mg}$, $*K_{ATP-Mg}$, and K_{Mg} (see Discussion).

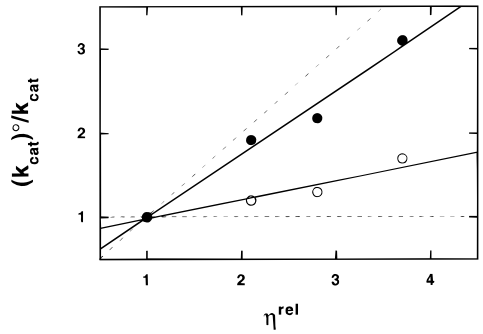

FIGURE 4: Effects of solvent viscosity on k_{cat} at 0.5 (○) and 10 (●) mM free Mg^{2+} using 2 mM ATP-Mg and 0.1−3.5 mM EAEIYEAIE. $(k_{cat})°/k_{cat}$ is the ratio of k_{cat} in the absence and presence of varying amounts of glycerol and η^{rel} is the relative solvent viscosity. The dotted lines represent slopes of 0 and 1, the theoretical limits for the data.

monitored as a function of peptide concentration using 2 mM ATP-Mg at 0%, 20%, 27%, and 35% glycerol in Mops buffer. The ratio of k_{cat} in the absence and presence of glycerol $[(k_{cat})°/k_{cat}]$ is plotted as a function of relative solvent viscosity (η^{rel}) in Figure 4 at 0.5 and 10 mM free Mg^{2+}. The plots are linear and have slope values of 0.75 ± 0.07 and 0.23 ± 0.04 at 0.5 and 10 mM free Mg^{2+}, respectively. At 10 mM free Mg^{2+}, no viscosity effect was observed on $k_{cat}/K_{peptide}$ (Table 2). These findings for k_{cat} and $k_{cat}/K_{peptide}$ are consistent with previously reported viscosity data for this peptide at 10 mM free metal and 3 mM ATP-Mg (*13*).

Since the concentration of ATP-Mg used in the viscosity experiment in Figure 4 is below K_{ATP-Mg} at 0.5 mM free Mg^{2+} (Table 1), the ratio of k_{cat}, now called $^{app}k_{cat}$, in the absence and presence of viscosogen was measured as a function of η^{rel} at several ATP-Mg concentrations to determine whether the nucleotide affects the slope term [i.e., $^{app}(k_{cat})^{\eta}$]. The effects of ATP-Mg concentration on $^{app}(k_{cat})^{\eta}$ are shown in Figure 5. The data were fit to a hyperbolic function to obtain $(k_{cat})^{\eta}$ and $(k_{cat}/K_{ATP-Mg})^{\eta}$ at low metal ion concentration (see eq 6 in Discussion). These fits are shown in Table 2. Also, the half-maximal concentration for the plot in Figure 5 is 3.7 ± 1.0 mM. The effects of solvent viscosity on k_{cat}/K_{ATP-Mg} at 10 mM free Mg^{2+} were determined by measuring initial velocities as a function of ATP-Mg concentration (0.1−2 mM) at saturating, fixed concentration of peptide (4 mM). A plot of $(k_{cat}/K_{ATP-Mg})°/(k_{cat}/K_{ATP-Mg})$ versus η^{rel} is linear (data not shown), and the slope value for this relationship, $(k_{cat}/K_{ATP-Mg})^{\eta}$, is shown in Table 2.

Table 2: Effects of Viscosity on the Steady-State Kinetic Parameters at 0.5 and 10 mM Free Magnesium[a]

parameters	$[Mg^{2+}]^{free}$ (mM) 0.5[b]	10[c]
$(k_{cat})^{\eta}$	0.88 ± 0.27	0.75 ± 0.07
$(k_{cat}/K_{peptide})^{\eta}$	−0.10 ± 0.08	−0.07 ± 0.06
$(k_{cat}/K_{ATP-Mg})^{\eta}$	0	−0.05 ± 0.10
K_d (peptide) (mM)[d]	≥2	2.2 ± 0.68
K_d (ATP-Mg) (mM)[d]	≥9	0.88 ± 0.26
k_3 (s^{-1})[e]	≥40	56 ± 17
k_4 (s^{-1})[e]	18 ± 6	19 ± 3

[a] The steady-state kinetic parameters were measured in 100 mM Mops, pH 7, at 23 °C. [b] The viscosity effects at this magnesium concentration were measured from v versus peptide substrate concentration (0.1−3.5 mM) plots at varied, fixed concentrations of ATP-Mg (1−10 mM). $(k_{cat})^{\eta}$ and $(k_{cat}/K_{ATP-Mg})^{\eta}$ were determined from extrapolations of $^{app}(k_{cat})^{\eta}$ to infinite and zero ATP-Mg concentrations, respectively. $(k_{cat}/K_{peptide})^{\eta}$ is an average value over all ATP-Mg concentrations. [c] The viscosity effects at this magnesium concentration were measured from v versus peptide substrate concentration (0.1−3.5 mM) plots at a fixed concentration of ATP-Mg (2 mM). [d] The K_d values for ATP-Mg and peptide were measured using eq 7. [e] The values of k_3 and k_4 were derived from the expression for the turnover number $[k_3k_4/(k_3 + k_4)]$ and $(k_{cat})^{\eta}$ by the following relationships: $k_4 = k_{cat}/(k_{cat})^{\eta}$ and $k_3 = k_{cat}/[1 - (k_{cat})^{\eta}]$ (*13*).

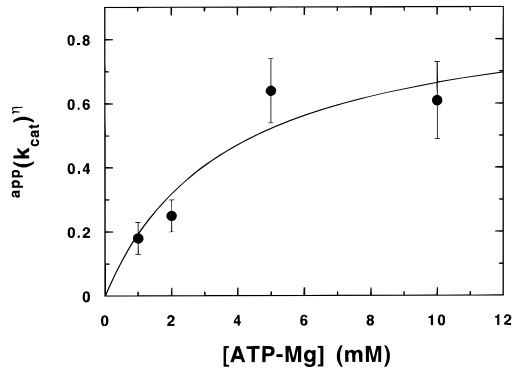

FIGURE 5: Effects of ATP-Mg concentration on $^{app}(k_{cat})^{\eta}$ at 0.5 mM free Mg^{2+}. $^{app}(k_{cat})^{\eta}$ was determined from the plots of $(^{app}k_{cat})°/^{app}k_{cat}$ versus η^{rel}. $^{app}k_{cat}$ was measured in the absence or presence of viscosogen using variable peptide substrate concentrations (0.1−3.5 mM) and fixed ATP-Mg concentrations of 1, 2, 5, and 10 mM.

DISCUSSION

To determine whether receptor and nonreceptor PTKs are broadly different with respect to their kinetic responses to metal ions and to investigate further the role of metal ions in catalysis, we studied the influence of free magnesium ions on the kinetic mechanism of a nonreceptor PTK, v-Fps, a member of the Fps/Fes family of nonreceptor PTKs. v-Fps is the oncogenic, retroviral product of the chicken c-Fps gene and has been shown to induce transformation in several cell lines including chicken embryo fibroblasts and Rat-2 cells (*18*−*20*). Most recently, it has been shown that the normal cellular forms of the Fps/Fes family are involved in the terminal differentiation of macrophages making this enzyme family an important component of the immune response (*21*). The members of the Fps/Fes family are composed of kinase

Scheme 1

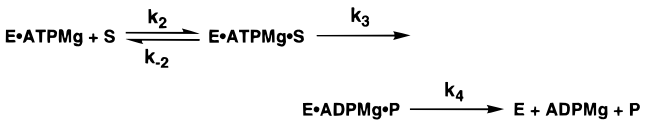

Scheme 2

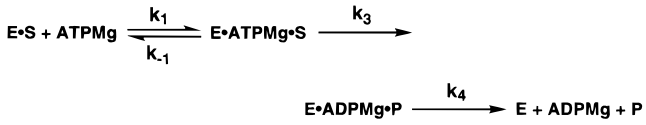

and SH2 (Src homology-2) domains at their C-termini but have large N-terminal regions with little sequence homology to other nonreceptor PTKs. Less is known about the function of the N-terminal compared to the C-terminal regions. The Fps/Fes family differs from the widely studied Src family in that they have no SH3 domains, lack N-terminal fatty acid modifications, are positively regulated by their SH2 domains (*22*, *23*), and are not negatively regulated by phosphorylation on their C-terminal tails.

Many PTKs have noncatalytic domains that influence activity and make difficult the kinetic analysis of the catalytic regions. The studies in this manuscript were performed on the isolated kinase domain of v-Fps, removing any potential influence from other noncatalytic regions of the enzyme. The analysis of this kinase domain and its comparison to the kinase domains of receptor PTKs such as FGFR will provide new insights into the nature of tyrosine phosphorylation and the conservation of mechanism within the protein kinase subclasses. We have demonstrated previously that the kinase domain of v-Fps (290 amino acids) can be overexpressed and purified as a fusion protein of glutathione-*S*-transferase (GST) in *E. coli* (*12*). This fusion protein is autophosphorylated (*12*) and possesses a turnover number close in value to that for PKA (*13*, *17*).

Effects of Free Magnesium on Turnover. Although high concentrations of free Mg^{2+} increase the activity of the kinase domain of v-Fps (Figure 1), there are no significant changes in k_{cat} over a wide concentration range of free metal (Table 1). The turnover rate for an enzyme is frequently a complex set of terms that define the net decomposition of the central complex and do not usually represent a single catalytic event. We have shown previously that turnover in v-Fps is controlled by both phosphoryl transfer and net product release at 10 mM free Mg^{2+} (*13*, *17*). Since turnover is directed by two observable steps, it is possible that free metal could change the rate of these two steps without significantly affecting k_{cat}. To determine the effects of the second metal ion on individual steps in the phosphorylation mechanism, we measured the effects of solvent viscosity on turnover at 0.5 and 10 mM free Mg^{2+} (Figure 4). At 10 mM metal and 2 mM ATP-Mg, GST-kin is bound with ATP-Mg so that the viscosity data can be interpreted according to Scheme 1, where the peptide substrate binds the E·ATP-Mg binary complex by the association and dissociation rate constants, k_2 and k_{-2}, respectively, the catalytic step, k_3, describes the favorable, unimolecular rate constant for the transfer of the γ phosphoryl group of ATP-Mg to the hydroxyl of tyrosine, and the final step, k_4, describes the net, bimolecular rate constant for the release of both products.

The rate constants for the individual steps in Scheme 1 can be derived based on the sensitivity of k_{cat} and $k_{cat}/K_{peptide}$ to added viscosogens using the Stokes−Einstein equation and the following relationships:

$$(k_{cat})^{\eta} = \frac{k_3}{k_3 + k_4} \tag{4}$$

$$(k_{cat}/K_{peptide})^{\eta} = \frac{k_3}{k_{-2} + k_3} \tag{5}$$

where $(k_{cat})^{\eta}$ and $(k_{cat}/K_{peptide})^{\eta}$ are the slopes for the plots of $(k_{cat})^{\circ}/k_{cat}$ and $(k_{cat}/K_{peptide})^{\circ}/(k_{cat}/K_{peptide})$ versus η^{rel}, respectively. Equations 4 and 5 predict that the slope values will fall between the limits of 0 and 1. We can use the rate expressions for k_{cat} $[k_3k_4/(k_3 + k_4)]$ and $k_{cat}/K_{peptide}$ $[k_2k_3/(k_{-2} + k_3)]$ and eqs 4 and 5 to determine the individual steps in Scheme 1. These values, reported in Table 2, indicate that k_3 and k_4 participate in limiting k_{cat}.

A reduced viscosity effect was measured at 0.5 mM free Mg^{2+} compared to that at 10 mM free Mg^{2+} (Figure 4). This effect is not due to a change in kinetic mechanism at lower metal concentrations since the concentration used in Figure 4 is below K_{ATP-Mg} and the turnover numbers measured in plots of initial velocity versus peptide substrate concentration provide only an apparent k_{cat} ($^{app}k_{cat}$). To determine the true viscosity effect on k_{cat} at low free metal, we measured the effects of viscosogen on $^{app}k_{cat}$ at several concentrations of ATP-Mg. The relative change in $^{app}k_{cat}$ as a function of η^{rel} $[(^{app}k_{cat})^{\eta}]$ varies hyperbolically with the total concentration of ATP-Mg (Figure 5). We interpret these data according to Scheme 2, where k_1 and k_{-1} are the association and dissociation rate constants for ATP-Mg to the binary E·S complex. In this scheme, eq 6 can be used to relate the effects of viscosity on $^{app}k_{cat}$ to the total concentration of ATP-Mg,

$$^{app}(k_{cat})^{\eta} = \frac{(k_{cat})^{\eta}[\text{ATP-Mg}] + (k_{cat}/K_{ATP-Mg})^{\eta}K_{ATP-Mg}}{[\text{ATP-Mg}] + K_{ATP-Mg}} \tag{6}$$

where $(k_{cat})^{\eta}$ is defined in eq 4, K_{ATP-Mg} is the observed K_m for ATP-Mg, and $(k_{cat}/K_{ATP-Mg})^{\eta}$ is equal to $k_3/(k_{-1} + k_3)$ at 0.5 mM free Mg^{2+}. This latter term represents the sensitivity of k_{cat}/K_{ATP-Mg} to solvent viscosity and has a form similar to that for eq 5. Extrapolation of this equation to infinite and zero ATP-Mg concentrations provides the true viscosity effect on k_{cat} $[(k_{cat})^{\eta}]$ and k_{cat}/K_{ATP-Mg} $[(k_{cat}/K_{ATP-Mg})^{\eta}]$. Furthermore, the concentration at which the half-maximal value for $^{app}(k_{cat})^{\eta}$ is achieved corresponds to K_{ATP-Mg}. Fitting of eq 6 to the data in Figure 5 provides these parameters which are listed in Table 2. Given the error limits in the primary data in Figure 5, we cannot accurately measure $(k_{cat}/K_{ATP-Mg})^{\eta}$, but since $^{app}(k_{cat})^{\eta}$ is small at low ATP-Mg concentrations, we presume that this parameter is near zero. On the basis of these limits, we report the lower limits for k_3 and the K_d values for ATP-Mg and peptide in Table 2. This analysis indicates that the effects of viscosity on turnover are similar at 0.5 and 10 mM free Mg^{2+} and there is no change in the rate-determining steps over this metal range. There is also a good correspondence between K_{ATP-Mg} derived from eqs 6 and 2 supporting this analysis. Finally,

since detailed kinetic studies cannot be performed below 0.5 mM free magnesium, it is possible that the turnover rate for the enzyme and the rates of either phosphoryl transfer or product release may be different below this amount of metal.

Magnesium Effects on Apparent ATP-Mg and Peptide Affinity. Extrapolation of the velocity data to zero and infinite free metal concentrations in Figure 1 indicates that the enzyme is active at stoichiometric amounts of ATP and Mg^{2+} but is activated approximately 20-fold beyond this by excess metal. Since the dissociation constant for ATP and Mg^{2+} is 14 μM (*15*), the true substrate for v-Fps is Mg-ATP, and magnesium levels above this must affect the kinetic parameters by binding to a secondary site. Two metal binding sites have been identified for the catalytic subunit of PKA using kinetic (*3*−*5*) and crystallographic (*7*, *24*) methods lending support to this interpretation for v-Fps. To determine the source of this activation, the complete steady-state kinetic parameters for the enzyme were measured over a wide range of free Mg^{2+}. While no large effect was found on turnover and only a 2-fold effect was measured on the K_m of the peptide substrate, a large effect was observed on the apparent affinity of ATP-Mg at varying free Mg^{2+} concentrations. K_{ATP-Mg} decreased from 3.6 to 0.22 mM between 0.5 and 10 mM free Mg^{2+} (Table 1), a 16-fold effect. This accounts for the observed effects of free Mg^{2+} on initial velocity since the steady-state kinetic parameters measured at 0.5, 10, and 20 mM free Mg^{2+} can be used to predict the velocity curve in Figure 1.

A thorough analysis of the effects of free Mg^{2+} on ATP-Mg affinity indicates that the binding of the second metal decreases the observed K_{ATP-Mg} from >8 to 0.10 mM, a minimum effect of 80-fold (Figure 3). Decreases in K_{ATP-Mg} have been observed for the catalytic subunit of PKA and FGFR at high levels of free Mg^{2+}. For PKA, K_{ATP-Mg} at zero free Mg^{2+} is approximately 0.2 mM and decreases 25-fold at high levels of free metal (*3*). For FGFR, K_{ATP-Mg} at low free Mg^{2+} is approximately 0.3 mM and decreases to 0.07 mM at high levels of free metal (10). These data are comparative to that for the kinase domain of v-Fps although the effects on v-Fps are considerably larger.

Magnesium Effects on the Dissociation Constants for ATP-Mg and Peptide. The K_m value for a peptide substrate oftentimes does not reflect the true affinity of the peptide substrate for the active site and may be either higher or lower than this value depending on the nature of the steps after formation of the central complex. The effects of solvent viscosity on the steady-state kinetic parameters can be used to determine the true effects of free Mg^{2+} on the dissociation constants for ATP-Mg and peptide. Since there is no viscosity effect on $k_{cat}/K_{peptide}$ (i.e., $k_3 \ll k_{-2}$) at either low or high metal concentrations, eq 7 can be used to relate the observed K_m to the true dissociation constant for peptide substrate (K_d):[2]

$$K_m = K_d[1 - (k_{cat})^\eta] \quad (7)$$

This analysis shows that the dissociation constant for the peptide substrate is higher than the K_m at either 0.5 or 10 mM free Mg^{2+} owing to the relative rates of k_3 and k_4 (Tables 1 and 2). While we can only place a lower limit on K_d at low metal owing to the error limits in the measurement of $(k_{cat})^\eta$, we do not have evidence that the peptide binds poorer at low compared to high Mg^{2+}.

Scheme 3

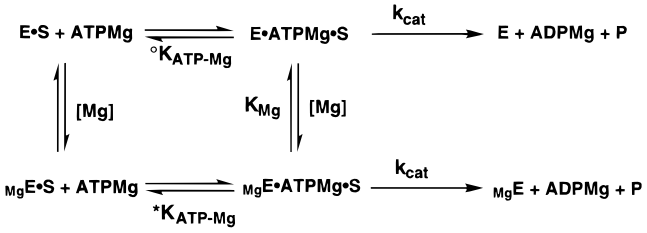

A viscosometric approach can also be used to measure the true affinity of ATP-Mg and the enzyme. Since no viscosity effect was measured for k_{cat}/K_{ATP-Mg}, eq 7 can be applied to determine the K_d for ATP-Mg.[2] Using this analysis, the K_d for ATP-Mg decreases more than 10-fold from 0.5 to 10 mM free Mg^{2+} (Table 2). Assuming that the viscosity effects are similar over all metal concentrations, the second metal must increase the binding affinity of ATP-Mg from >32 to 0.4 mM, a minimum 80-fold effect. Therefore, in the absence of the second metal, a large energetic barrier exists for the stable association of the nucleotide and the enzyme. The second Mg^{2+} greatly reduces this barrier. Finally, the negative binding synergism between ATP-Mg and peptide at low metal concentrations which is relieved somewhat at higher metal concentrations (Table 1 and Figure 2) supports a constructive role for the second metal on ATP-Mg binding. We propose that this latter phenomenon is due to a reduction in charge repulsion between ATP-Mg and peptide, polyanionic molecules at neutral pH. While this effect is not accompanied by an increase in peptide affinity at high metal, there could be other metal-dependent changes that compensate for this.

Affinity of the Second Magnesium Ion. The dissociation constant for the second metal (K_{Mg}) derived from the influence of free Mg^{2+} on K_{ATP-Mg} (Figure 3) reflects the true affinity of the ion in the presence of both ATP-Mg and peptide. Under conditions of high peptide concentration, the role of Mg^{2+} in the kinetic mechanism can be summarized in Scheme 3, where $^\circ K_{ATP-Mg}$ and $^* K_{ATP-Mg}$ represent K_{ATP-Mg} in the absence and presence of the second metal and K_{Mg} is the dissociation constant for Mg^{2+} in the ternary complex. Equation 3 is derived from this scheme and describes the free Mg^{2+} dependence on the observed K_{ATP-Mg}. Fitting of this equation to the data in Figure 3 places an upper limit of 0.3 mM on the affinity of the second metal ion in GST-kin (K_{Mg}). In contrast to this dissociation constant, the observed dissociation constant for Mg^{2+} is 13 mM under conditions of 0.2 mM ATP-Mg and 1 mM peptide (Figure 1). This value is perturbed from the true affinity of Mg^{2+} based on the difficulty of achieving the ternary complexes, $_{Mg}$E·ATP-Mg·S and E·ATP-Mg·S, at lower metal concentrations when ATP-Mg binds poorly. Despite this, the observed K_{ATP-Mg} and $K_{peptide}$ could be used to predict the initial velocity versus Mg^{2+} curve in Figure 1. Finally, the affinity of the second metal in the kinase domain of v-Fps is significantly higher than that for PKA or the PTKs, Csk,

[2] There are small, negative effects of viscosogens on $k_{cat}/K_{peptide}$ at 0.5 and 10 mM free Mg^{2+} and on k_{cat}/K_{ATP-Mg} at 10 mM free Mg^{2+} (Table 2). Since the error limits on these slope values [$(k_{cat}/K_{peptide})^\eta$ and $(k_{cat}/K_{ATP-Mg})^\eta$] are large, we treat these values as zero.

FGFR, and Src (*3*, *10*). By monitoring the effects of free Mg^{2+} on either V_{max} or K_{ATP-Mg} for these enzymes, the kinase domain of v-Fps binds the second metal a minimum of 3−9-fold more tightly.

CONCLUSIONS

We have shown using detailed kinetic approaches that the kinase domain of v-Fps supports the binding of two magnesium ions. The first metal is essential for catalysis but does not permit the stable association of ATP-Mg (K_d > 32 mM). Since the affinity of the second metal ion is less than 0.3 mM and kinetic experiments cannot be performed below this amount, it is possible that free Mg^{2+} can affect phosphoryl transfer and product release, but the first metal is sufficient for phosphoryl transfer. Nonetheless, the prominent role for free Mg^{2+} is to assist ATP-Mg binding by decreasing the dissociation constant by, at least, 80-fold. These effects contrast sharply with those for two nonreceptor PTKs, Src and Csk, where the second magnesium ion is apparently essential for catalysis and does not influence the binding of ATP-Mg (*10*). Although there is no three-dimensional structure for the kinase domain of v-Fps, the X-ray structure of the trisphosphorylated insulin receptor kinase with an ATP analogue and peptide substrate bound indicates that metal coordination is significantly different than that observed in PKA. Nonetheless, the metal-induced kinetic profile for v-Fps, a nonreceptor PTK, is surprisingly more consistent with the receptor PTK, FGFR, where increasing free Mg^{2+} enhances ATP-Mg binding. We propose that our results indicate either that v-Fps is a unique member of the nonreceptor PTK family and, thus, responds differently to metals or that the noncatalytic domains of v-Fps influence this metal effect.

REFERENCES

1. Adams, J. A., and Taylor, S. S. (1993) *Protein Sci. 2*, 2177−2186.
2. Kee, S. M., and Graves, D. J. (1987) *J. Biol. Chem. 262*, 9448−9453.
3. Cook, P. F., Neville, M. E., Vrana, K. E., Hartl, F. T., and Roskoski, J. R. (1982) *Biochemistry 21*, 5794−5799.
4. Kong, C.-T., and Cook, P. F. (1988) *Biochemistry 27*, 4795−4799.
5. Armstrong, R. N., Kondo, H., Granot, J., Kaiser, E. T., and Mildvan, A. S. (1979) *Biochemistry 18*, 1230−1238.
6. Granot, J., Kondo, H., Armstrong, R. N., Mildvan, A. S., and Kaiser, E. T. (1979) *Biochemistry 18*, 2337.
7. Zheng, J., Knighton, D. R., Ten Eyck, L. F., Karlsson, R., Xuong, N.-h., Taylor, S. S., and Sowadski, J. M. (1993) *Biochemistry 32*, 2154−2161.
8. Zhou, J., and Adams, J. A. (1997) *Biochemistry 36*, 15733−15738.
9. Qamar, R., Yoon, M.-Y., and Cook, P. F. (1992) *Biochemistry 31*, 9986−9992.
10. Sun, G., and Budde, R. J. A. (1997) *Biochemistry 36*, 2139−2146.
11. Vicario, P. P., Saperstein, R., and Bennun, A. (1988) *Arch. Biochem. Biophys. 261*, 336−345.
12. Gish, G., McGlone, M. L., Pawson, T., and Adams, J. A. (1995) *Protein Eng. 8*, 609−614.
13. Wang, C., Lee, T. R., Lawrence, D. S., and Adams, J. A. (1996) *Biochemistry 35*, 1533−1539.
14. Adams, J. A., and Taylor, S. S. (1992) *Biochemistry 31*, 8516−8522.
15. Martell, A. E., and Smith, R. M. (1977) *Critical Stability Constants*, Vol. 3, Plenum, New York.
16. Shoemaker, D. P., and Garland, C. W. (1962) *Experiments in Physical Chemistry*, 2nd ed. McGraw-Hill, New York.
17. Adams, J. A. (1996) *Biochemistry 35*, 10949−10956.
18. Foster, D. A., Shibuya, M., and Hanafusa, H. (1985) *Cell 42*, 105−115.
19. Foster, D. A., and Hanafusa, H. (1983) *J. Virol. 48*, 744−751.
20. Feldman, R. A., Wang, E., and Hanafusa, H. (1983) *J. Virol. 45*, 782−791.
21. Areces, L. A., Sbarba, P. D., Jucker, M., Stanley, E. R., and Feldman, R. A. (1994) *Mol. Cell. Biol. 14*, 4606−4615.
22. Koch, C. A., Moran, M., Sadowski, I., and Pawson, T. (1989) *Mol. Cell. Biol. 9*, 4131−4140.
23. Hjermstad, S. J., Peters, K. L., Briggs, S. D., Glazer, R. I., and Smithgall, T. E. (1993) *8*, 2283−2292.
24. Madhusudan, Trafny, E. A., Xuong, N.-h., Adams, J. A., Ten Eyck, L. F., Taylor, S. S., and Sowadski, J. M. (1994) *Protein Sci. 3*, 176−187.

BI9812672